SOCIETY FOR SCIENCE AND EDUCATION UNITED KINGDOM

JBEMi JOURNAL OF BIOMEDICAL ENGINEERING AND MEDICAL IMAGING

ISSN: 2055-1266
VOLUME 3 ISSUE 1

Development of Plantar-Pressure Estimation Method Based on Continuous Plantar Images

Yuka Iijima, Koji Imai, Takeshi Yamakoshi, Hiroshi Mizoguchi, and Hiroshi Takemura
Department of Mechanical Engineering, Faculty of Science and Technology,
Tokyo University of Science, Tokyo, Japan
7514604@ed.tus.ac.jp

ABSTRACT

We propose a novel plantar-pressure estimation method using high-resolution plantar images. The proposed method can calculate the plantar-pressure distribution, ground reaction force, and center-of-pressure (COP) trajectory based on the weight of a subject, contact-area size, and brightness distribution of a plantar image captured by a high-speed camera. Four experiments are conducted to evaluate the proposed method. First, the relationship between the contact area/pressure condition and brightness distribution of the image is investigated. The result shows that the brightness increases according to the area size under the same pressure condition. Second, the plantar-pressure distribution calculated by the proposed method is compared with that of commercial pressure sensors. The results demonstrate that the plantar-pressure characteristics of the subject even in a small region are unambiguously represented. Third, the ground reaction force estimated by the proposed method is compared with that of the commercial force plate. The root mean square error (RMSE) is 16% of the maximum ground reaction force. The COP trajectory calculated by the proposed method is compared with the result obtained using the force plate. The averages of COP.x and COP.y RMSEs are calculated as 6.0 and 28.6 mm, respectively, which suggest that the proposed method can calculate the pressure distribution, ground reaction force, and COP trajectory. We apply the proposed method to a developed caterpillar-type transparent treadmill and demonstrate that the proposed method can be used for continuous plantar-pressure distribution measurement.

Keywords: Plantar image; Plantar pressure; Brightness distribution; Image processing; CaTTaP

1 Introduction

Plantar-pressure distribution is one of the well-known parameters that many researchers and therapists have been measuring and using for gait evaluation. Many types of plantar-pressure measurement systems have been proposed. The major systems are classified into three types according to the sensing method such as ink, image, or electronic sensor. The ink-type system measures the plantar pressure using the intensity of the static data obtained by walking over a paper with the soles covered with powder [1, 2]. The ink-type system cannot measure dynamic data. The image-type system calculates the plantar-pressure distribution based on the brightness of the grayscale plantar image captured by a camera located under a “barograph device” with a plain glass plate covered with a thin seat of white

DOI: 10.14738/jbemi.31.1866
Publication Date: 22nd February 2016
URL: http://dx.doi.org/10.14738/jbemi. 31.1866

deformable plastic [3]. In spite of the active research in the 1980s, the use of this type did not widely spread because of the spatial/time resolution and camera cost at that time. However, information derived from plantar images serves as a useful, reliable, and objective component in gait analysis. Currana et al. reported the differences between the joint angles of the ankle based on dynamic and static plantar images [4]. Lin et al. constructed a system to investigate the relationship between static balance and foot structure of children using a footprint image [5]. Hawes et al. measured the foot arch from the ratio of a plantar bearing area to the area of the foot arch [6]. Nakajima et al. proposed a method for personal identification based on plantar shape [7]. Shiina et al. suggested a relationship between plantar skin deformation and gait stability based on plantar images [8]. Form the above studies, although plantar image has great potential for analyzing and understanding the gait, methods to obtain the plantar image are seldom used in clinical applications. Today, almost all researchers who analyze plantar-pressure data use electronic sensors. These sensors come in many types such as mat [9], treadmill [10], insole [11], and small three-seal types [11]. However, conventional sensors do not have sufficient resolution to estimate the pressure of small regions such as the toes.

We focus on the resolution of a captured image and propose a new method that clearly estimates the high-resolution plantar-pressure distribution based on a plantar image.

2 Imaging Plantar-Pressure Estimation Method

2.1 Plantar image

We propose a new method that estimates the plantar-pressure distribution using the brightness distribution of a grayscale plantar image “directly” captured during walking (Figure 1) without any seat, in contrast to the conventional methods [3]. The captured image clearly shows the change in the brightness distribution.

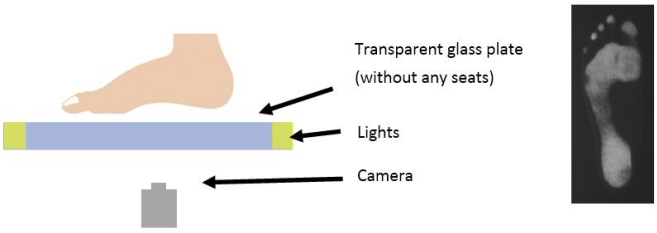

Figure 1 Capture method and the captured image

In the plantar image, the high-pressure area of the heel displays high brightness, whereas the low-pressure area in the arch area displays low brightness. This brightness change occurs because greater pressure causes closer contact between the skin and the glass plate, and the total internal reflection within the glass and the rough skin surface increases (Fig. 2). In a previous research [12], the correlation between pressure and brightness of the plantar contact area was high ($R > 0.9$), and the brightness increased according to the pushed vertical force according to a quadratic function.

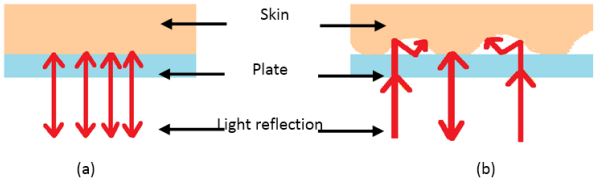

Figure 2 Light reflection of two types. (a) High pressure. (b) Low pressure

2.2 Image processing

To clearly show the brightness distribution of the plantar image, the grayscale images are converted to pseudo colors, as shown in Figure 3.

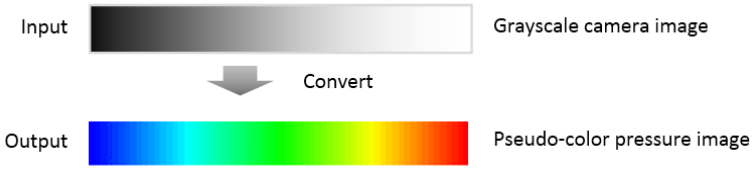

Figure 3 Conversion diagram of the proposed method

To generate a clear pseudo-color image, the brightness of the plantar image is normalized by Equation (1). *Max* and *Min* denote the maximum and minimum brightness of all images. Figure 4 shows the brightness change parameter from the input brightness value to the pseudo-color pressure image.

$$\text{Normalized brightness} = \text{Brightness} * 255/(Max - Min) \quad (1)$$

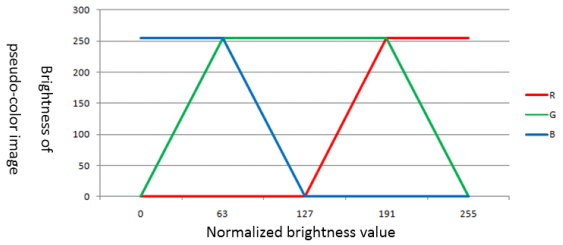

Figure 4 Diagram of the changing RGB channel to generate a pseudo-color image

The pressure on each pixel is calculated as $P(x,y)$ using Equations (2) and (3). (x,y) denotes the coordinate in the anterior–posterior and the medial–lateral axes. *Area* denotes the contact area [pixel], and *Normalized area* denotes the contact area normalized by the maximum size of all data [*Max area* (pixel)]. α and β are weighting parameters to correct the influence of the normalized area and brightness size on the pressure. The total vertical force on the whole sole is calculated using the sum of $P(x,y)$ [expressed by Equation (4)]. *Fz.pm* denotes the force estimated by the proposed method. *Width* and *Height* denote the width and height of the image. The ground reaction force during walking shows bimodal peaks (Fig. 5); two peaks show approximately 110% of the body weight, and the nadir shows approximately 80% of the body weight [13]. By using these characteristics, each of the weighting parameters (α and β) in the first and second terms (shown in Fig. 5) are calculated.

$$p(x,y) = brightness^2 \times \frac{(1 - \alpha \times Normalized\ area)}{\beta} \quad (2)$$

$$Normalized\ area = Area\ /\ Max\ area \quad (3)$$

$$Fz.pm = \sum_{0}^{width} \sum_{0}^{height} brightness^2 \times \frac{(1 - \alpha \times Normalized\ area)}{\beta} \quad (4)$$

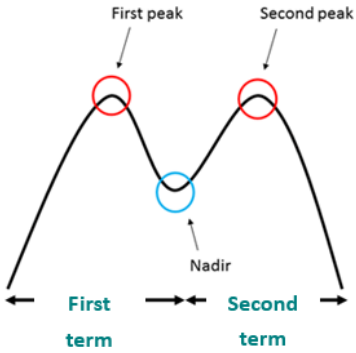

Figure 5 Two terms of the ground reaction force

The center-of-pressure (COP) coordinates are calculated by Equations (5) and (6). (*x*,*y*) denotes the coordinate in the anterior–posterior and the medial–lateral axes.

$$COP.x = \frac{\sum_0^{width} x \times p(x,y)}{\sum_0^{height} \sum_0^{width} p(x,y)} \quad (5)$$

$$COP.y = \frac{\sum_0^{height} y \times p(x,y)}{\sum_0^{height} \sum_0^{width} p(x,y)} \quad (6)$$

3 Estimation Experiments of the Proposed Method

3.1 Experimental device

Figure 6 shows the measurement device to capture the plantar image and measure the force. This device is composed of a camera (Point Grey Research, Inc., GZL-CL-41C6M-C, 2048 × 2048 [pixel], 150 fps), a transparent glass plate, and the force sensors (Tec Gihan Co., Ltd., TF-4060-G, 5000 fps).

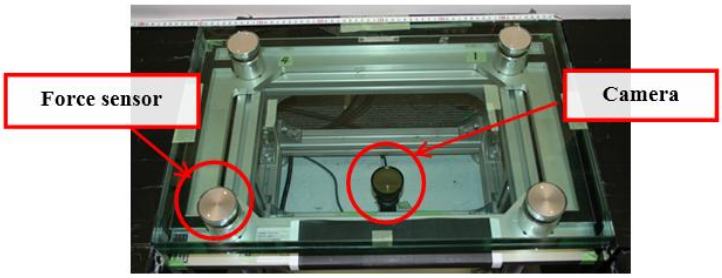

Figure 6 Measurement device (top view)

3.2 Evaluation of the relationship between brightness and contact area

The relationship between the contact area/pressure condition and brightness distribution of the image under the same pressure condition is determined. Three seats made of polyvinyl chloride, whose stiffness is similar to a human heel, are used for the measurement, instead of a human foot. Three types of brightness distribution in same pressure conditions are compared, as shown in Fig. 7, i.e., brightness in the contact area of the following: (1) 10-kg weight on a seat (25 × 66 × 14 mm^3), (2) 20-kg weight on a seat (50 × 66 × 14 mm^3), and (3) 30-kg weight on a seat (75 × 66 × 14 mm^3). The pressed images are captured by the camera located under the plate.

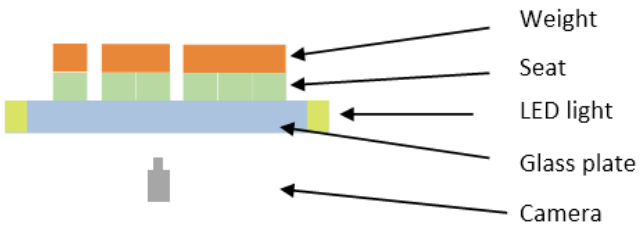

Figure 7 Experimental conditions under the same pressure distribution

Figure 8 shows the trimmed images (size: 50 × 50 pixels) of the seat subjected to the three weight patterns. The brightness averages are calculated as 91, 114, and 128. This result shows that the brightness under the same area pressure increases according to the size of the area.

Figure 8 Part of each seat image

3.3 Evaluation of the plantar-pressure distribution

The plantar-pressure distribution calculated by the proposed method was compared with that of the commercial pressure distribution sensors. Fig. 9 shows the data of the captured images (a), the results of the proposed method (b), and the results of the conventional sensors (LL sensor, Xiroku Inc.) (c).

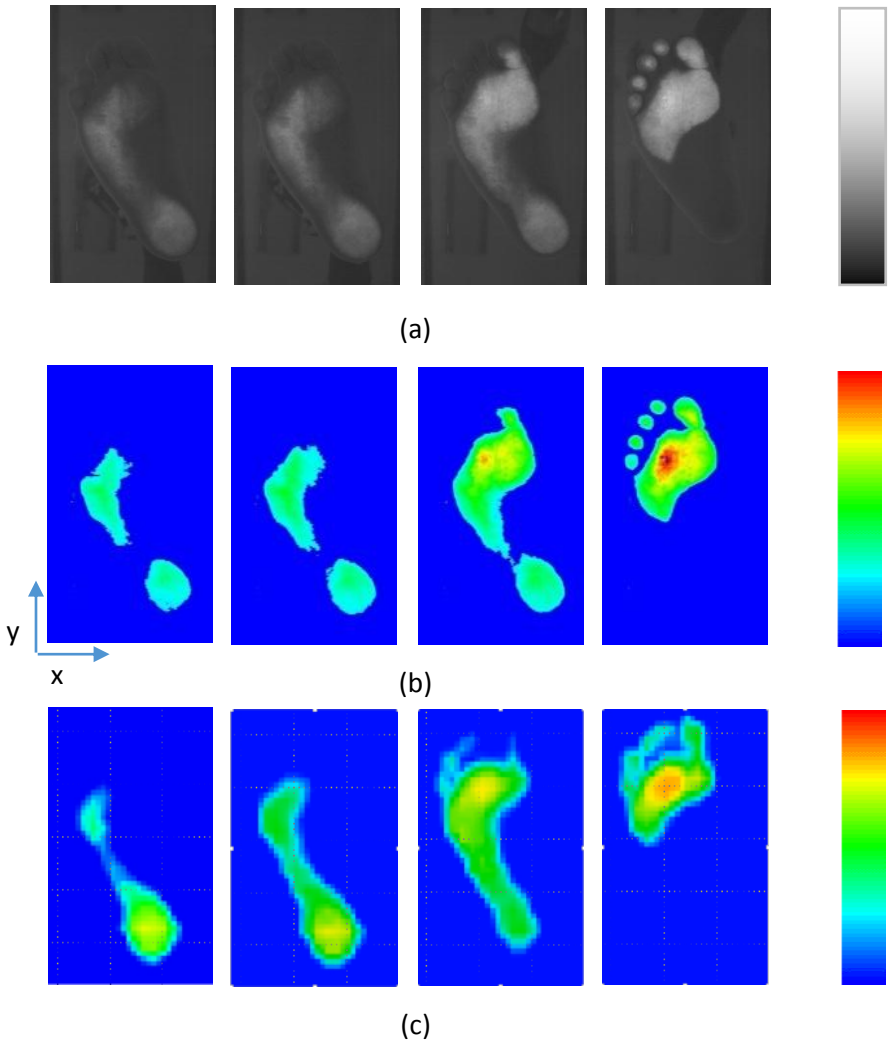

Figure 9 Data of the (a) captured images, (b) results of the proposed method, and (c) results of the conventional sensors

3.4 Accuracy of the ground reaction force

The ground reaction force estimated by the proposed method was compared with that of the commercial force plate. In this experiment, four healthy subjects (Ave. 23.0 $\pm$ 2 years old) were recruited, and 5400 clear plantar images were obtained during walking. Fig. 10 shows the ground reaction force measured by the force sensor (*Fz.fp*) and the proposed method (*Fz.pm*) for a subject. *Fz.pm* indicates the characteristic of bimodal peaks for *Fz.fp*. The average root mean square error (RMSE) calculated by comparing *Fz.pm* and *Fz.fp* is 16%.

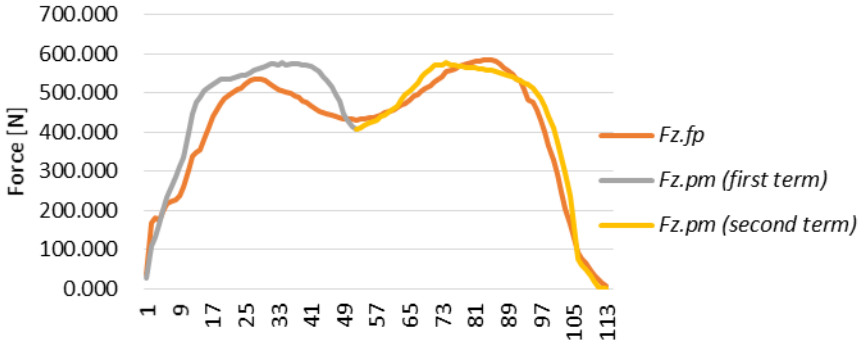

Figure 10 Forces measured by the force plate and the proposed method

3.5 Accuracy of COP

The COP trajectory calculated by the proposed method was compared with that calculated using the force plate. Fig. 11 shows the RMSEs and standard deviation of the COP calculated using the force sensors and the proposed method. The average *x*-axis RMSE is 6.0 mm, and the average *y*-axis RMSE is 28.6 mm. These results show that the accuracy of the COP calculation does not depend on the arch type.

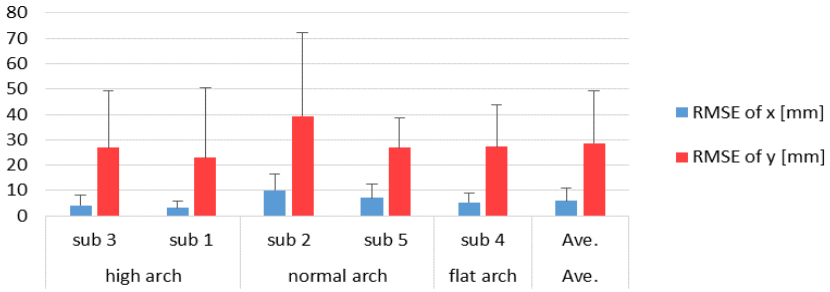

Figure 11 RMSEs of the COP for each subject

Figure 12 shows the plantar image in the high-accuracy (a) and low-accuracy (b) groups of the calculated COP. The contact area in the image in the high-accuracy group is clearer than that in the low-accuracy group. These images suggest that the accuracy of the proposed method depends on the condition of the sole.

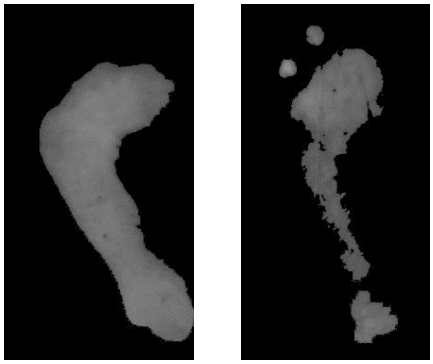

Figure 12 Plantar images of the (a) high- and (b) low-accuracy groups

4 Discussion

The first experiment proved the necessity of correcting the pressure expression by the normalized area. The second experiment showed that the pressure distribution calculated by the proposed method is quantifiably similar to that calculated by the conventional electronic sensor system. The image provided higher resolution data (approximately 4900 pixels/cm^2 depending on the image sensor of the camera) than the pressure distribution sensor (one sensing detector/cm^2). The results show that the pressure distribution in the small region such as toes, which cannot be calculated by the existing sensor [the highest resolution of commercial pressure distribution sensing system: four sensing detector/cm^2 (F-scan II, Nitta Co.)] can be calculated by the proposed method. Such high resolution makes the analysis of a floating-toe walk easier. The third experiment showed that the average RMSE in calculating the force is 16% of the maximum force. Compared with the 10% accuracy of the force plate, the proposed method needs further improvement. However, the contact area and plantar pressure, which cannot be measured by the force plate, can be measured by the proposed method. The last experiment showed that the average RMSE of the COP does not depend on the arch but on the condition of the sole of the subject. According to the experimental results, images in a normal condition and a changed condition (such as soft skin by bathing the sole of the subject in tepid water for 5 min) are captured and compared in terms of the contact area. Fig. 13(a) shows the image in a normal condition, and Fig. 13 (b) shows the image in a soft condition. In Fig. 13(c), the light blue, dark blue, and pink regions show each area listed in Table 1. Fig. 13(c) and Table 1 show that the soft sole is captured much clearer than the hard one because the accuracy of the proposed method also depends on the sole condition of the subject. This result suggests that softening the sole of the subject by footbath is one of the best ways to make the proposed method more accurate.

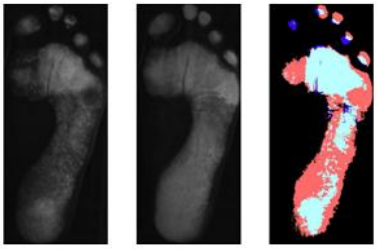

Figure 13 Plantar images of (a) normal condition, (b) soft condition, and (c) comparison result

Table 1 Area ratio in each region

	A contact and B contact	49.6 %
	A contact and B non-contact	3.3 %
	A non-contact and B contact	51.5 %

In addition, we developed a new system to analyze the gait using a new treadmill—the caterpillar-type transparent treadmill (CaTTaP) [14] (as shown in Fig. 14)—that continuously captures plantar images

during walking. Using the CaTTaP, gait parameters such as step length, step width, plantar skin deformation, contact area, and sole shape are calculated based on the clear dynamic plantar images at any steps, which are difficult to obtain using other devices. Application of the proposed method to CaTTaP (as shown in Fig. 15) makes the estimation of continuous plantar-pressure distribution available for any steps.

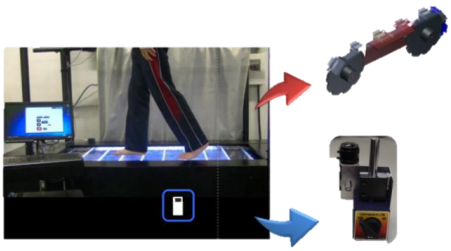

Figure 14 CaTTaP

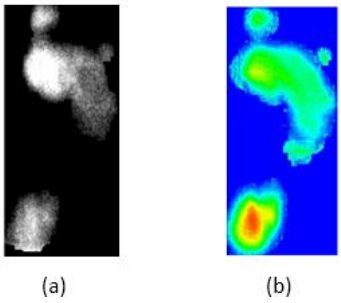

Figure 15 Images by CaTTaP. (a) Original image and (b) pseudo-color pressure image by the proposed method

5 Conclusion

This paper presented a novel plantar-pressure estimation method using high-resolution plantar images. The proposed method can calculate the plantar-pressure distribution, ground reaction force, and COP trajectory based on the weight of a subject, size of the contact area, and brightness distribution of the plantar image captured by a high-speed camera located under a transparent glass plate. Four experiments were conducted to evaluate the proposed method, and the results suggested that the proposed method can potentially calculate the pressure distribution, ground reaction force, and COP trajectory with high accuracy. We applied the proposed method to the developed CaTTaP and demonstrated that it is available for continuous plantar-pressure distribution measurement. We confirmed that CaTTaP is one of the best gait analysis systems available for clinical use.

REFERENCES

[1] Masahito, A., et al., *A gait analysis system using foot path images*, Journal of the Japan Society for Precision Engineering, 2008. 74(12). p. 1318–1324.

[2] Silvino, N., et al., *The Harris and Beath footprinting mat: Diagnostic validity and clinical use*, Clinical Orthopaedics and Related Research, 1980. 151: p. 265–269.

[3] Betts, R.P., et al., *Critical light reflection at a plastic/glass interface and its application to foot pressure measurements*, Journal of Medical Engineering and Technology, 1980. 4(3) : p. 136-142.

[4] Currana, S.A., et al., *Dynamic and static footprints: Comparative calculations for angle and base of gait*, The Foot, 2005. 15(1): p. 40–46.

[5] Lin, C.H., et al., *Development of a quantitative assessment system for correlation analysis of footprint parameters to postural control in children*, Physiological Measurement, 2006. 27(2): p. 119–130.

[6] Hawes, M.R., et al., *Footprint parameters as a measure of arch height*, Foot Ankle, 1992. 13(1): p. 22–26.

[7] Nakajima, K., et al., *Footprint-based personal recognition*, IEEE Transactions on Biomedical Engineering, 2000. 47(11): p. 1534–1537.

[8] Shiina, T., et al., *Measurement of undetectable walking feature by appearance based on plantar skin deformation*, The 15th International Conference on Biomedical Engineering, 2013. p. 116–119.

[9] Middleton, L., et al., *A floor sensor system for gait recognition*, Automatic Identification Advanced Technologies, 2005. 5(7): p. 171–176.

[10] Alon, K., et al., *Quantifying gait impairment using an instrumented treadmill in people with multiple sclerosis*, Hindawi Publishing Corporation ISRN Neurology, 2013. Article ID 867575, 6 pages.

[11] Peter, R., et al., *In-shoe plantar pressure measurement: A review*, The Foot, 1992. 2(4): p. 185–194.

[12] Yuka, I., et al., *Measurement of plantar pressure distribution based on grayscale plantar images*, The 8th Asian-Pacific Conference on Biomechanics, 2015. PS8-1.

[13] Jacquelin P., et al., *Gait analysis: Normal and pathological function*, Slack Inc. (2010).

[14] Yuka, I., et al., *Development of gait analysis system based on continuous plantar images obtained using CaTTaP device*, Advanced Biomedical Engineering, 2015. 4(0): p. 119–125.

